# Chemical foaming extrusion of poly(lactic acid) with chain-extenders: Physical and morphological characterizations

J.M. Julien, J.-C. Quantin, J.-C. Bénézet, A. Bergeret, M.F. Lacrampe, P. Krawczak

# Chemical foaming extrusion of poly(lactic acid) with chain-extenders: Physical and morphological characterizations

J.M. Julien [a,b,c], J.-C. Quantin [c,*], J.-C. Bénézet [c], A. Bergeret [c], M.F. Lacrampe [a,b], P. Krawczak [a,b]

[a] Univ. Lille Nord de France, 59000 Lille, France
[b] Ecole des Mines de Douai, Department of Polymers and Composites Technology & Mechanical Engineering, 941 Rue Charles Bourseul, BP 10838, 59508 Douai, France
[c] Ecole des Mines d'Alès, Centre C2MA, 6 Avenue de Clavières, 30319 Alès Cedex, France

A B S T R A C T

The effects of an epoxide-based chain-extender (CE) on the properties of poly(lactic acid) (PLA) foams obtained by chemical foaming extrusion using 4 wt.% of chemical foaming agent (CFA) were studied. PLA/CE blends with different weight ratios of CE were initially processed using a co-rotating twin-screw extruder. PLA/CE foams were then produced using a single-screw extruder. Various PLA/CE foams characterizations, including solution viscosity, thermal properties (DSC, TGA), cellular structure (void fraction, cell size, open cell content), mechanical and dynamic rheological behaviors, were investigated. Results show that the addition of CE enhances the viscosimetric average molecular weight and rheological properties (viscosity and storage modulus) of PLA, but it has no significant effects on the thermal properties of PLA, except the occurring of a cold crystallization. The CE incorporation also led to a decrease in the void fraction of cellular PLA, in the cell size and in the open cell content and to an increase in the cell density. Furthermore, the tensile mechanical properties such as yield stress and elongation at break of cellular materials increased with the addition of CE.

*Keywords:*
Poly(lactic acid)
Extrusion foaming
Chemical foaming agent
Epoxide based chain-extender
Cell morphology

## 1. Introduction

One way to overcome the issues related to the management of waste plastic parts, to the oil price fluctuations and to the gradual depletion of fossil resources is to use biodegradable polymers derived from renewable resources, called bio-based and biodegradable polymers. Poly(lactic acid) (PLA) is one of the most promising polyesters for this purpose [1]. Therefore, it generates a huge scientific and industrial literature [2–5], especially because its mechanical properties are equivalent or even higher to those of traditional polymers [6]. It is synthesized from L- and D-lactic acid, which are themselves produced from the fermentation of dextrose provided by starch hydrolysis (starch can be extracted from corn, wheat, potatoe or sugar cane for example), either by ring-opening polymerization or by condensation polymerization depending on the targeted molecular weight [2,7,8]. In non-medical industries, PLA is mainly used in packaging applications [9] because of its biodegradability [10]. The biocompatibility and bioresorbability of PLA make it also particularly well-suited in the biomedical industries for high added value products [4,7,11] such as bone plates, bone screws, drug delivery and tissue repair systems [12–15]. Moreover, PLA can be processed by traditional plastic processing techniques for the production of films, fibers, extruded or injection molded parts or foams [7,16]. For this latter case, obtaining PLA-based foam products is of major industrial interest, in order to reduce carbon footprint and

* Corresponding author. Tel.: +33 4 66 78 53 46; fax: +33 4 66 78 53 65.
*E-mail address:* jean-christophe.quantin@mines-ales.fr (J.-C. Quantin).

environmental impact by plastic parts lightening at equivalent end-use performances.

Physical and chemical foaming agents [17–19] can be used for PLA. Physical foaming is achieved by gas injection (for example nitrogen) in the molten PLA. Chemical foaming is achieved by blending solid endothermic or exothermic chemical foaming additives (so-called CFA) with the polymer matrix. The result is the release of a gas and the growing of cells while the temperature increases leading to a reduction in density of about 50% [17–19]. This reduction depends on processing conditions such as screw speed, die geometry and processing temperature [20]. A previous study [1] assessed the optimization of the PLA chemical foaming conditions based on a maximal void fraction criterion. Using an endothermic chemical foaming agent, an homogeneous cell structure with low open cell content (27%) corresponding to a void fraction of 47% was obtained in optimized processing conditions. Nevertheless this study showed also that the low melt strength of the PLA [21,22] could be considered as a limiting factor to foaming. In order to overcome this drawback three ways of PLA modification were explored in literature: The first way consists in combining the effect of irradiation (electron beam or $\gamma$-ray) and of a crosslinking agent (such as a polyfunctional monomer, for example TAIC (triallyl isocyanurate which is commonly used)). The second one will compensate the degradation of the polymer induced by the first one [3,23–26]. The second way consists in adding melt strength enhancers with high molecular weights (acrylic, ...) in PLA. That will enhance the elongation viscosity of the melt, resulting from entanglements [27]. The third and last way reported in literature consists in adding a chain-extender combined with a crosslinking agent (peroxide or isocyanate) to induce chain scission, extension, crosslinking, or any combination of the three, depending on the chain extender amount, resulting in the variation of the gelation level of the material [28,29]. Di et al. [29] have modified a PLA (L-lactide > 92%) by sequentially adding different ratios of 1,4-butane diol and 1,4-butane diisocyanate as chain-extenders using an internal mixer at 170 °C. The results show higher molecular weights and rheological properties (viscosity and moduli). The higher viscosity and elasticity of the modified PLA samples allowed the production of physical foams (using a mixture of $CO_2$ and $N_2$ as foaming agent) with a smaller cell size, a higher cell density and a lower density compared to the unmodified PLA. Other chain-extenders with di-functional ($f_n = 2$) compounds such as carboxylic acid, hydroxyl, amine, anhydride and epoxide lead to a lower enhancement in molecular weight compared with multi-functional compounds ($f_n \geqslant 3$). This is because di-functional compounds will only link two end groups, thereby leading to a linear polymer [30]. Thus, the use of chain-extenders with multi-functional compounds has become an attractive means to increase their efficiency. These products lead to a branched structure which can be useful in a polymer foaming process, because they allow the polymer to withstand the triaxial deformation that occurs during the cell growth. Among multi-functional chain-extenders, the multi-functional epoxide based chain-extenders have a very broad processing window, which can be used in traditional extrusion or injection-molding equipments without vacuum or catalysts [4]. The reaction mechanisms of epoxide-based chain-extenders in reactive extrusion have been largely described in the literature [31–35]. But up to now, no study has been reported concerning the use of these components to assist chemical foaming extrusion of PLA matrices.

In this context, the present study focuses on the chemical foaming extrusion of modified PLA with an epoxide-based chain-extender. The effects of chain-extenders on the void fraction, the cell morphology (cell size, cell density, cell-wall thickness), the thermal and mechanical properties of PLA foams are investigated. The main objective is to perform cellular materials with better controlled characteristics (density, cell morphology and mechanical properties) by varying the amount of chain extender.

## 2. Experimental

### 2.1. Materials

A commercial grade of linear polylactic acid (PLA 7000D®, NatureWorks® LLC, USA, containing 6.4% of D-lactide (determined by polarimetric analysis by Max Mousseron Institute of Biomolecules, UMR CNRS 5247, University of Montpellier 1, University of Montpellier 2, Faculty of Pharmacy, Montpellier, France) was used in this study, in combination with an endothermic chemical foaming agent (CFA, Hydrocerol® CT3108, Clariant Masterbatches, France) containing sodium bicarbonate and citric acid. The gas yield of the CFA is around 50 ml/g (supplier data). A CFA amount of 4 wt.% was incorporated into the PLA according to a previous work [1]. The chain-extender (so-called CE, CESA-Extend BLA0050109-ZN, Clariant Masterbatches, France) is a multi-functional epoxide-based chain-extender (Fig. 1), composed of a styrene–acrylic oligomer with a number-averaged molecular weight ($M_n$) around 6800 g/mol and a high number-average functionality ($f_n \sim 9$) (supplier data). This agent was especially designed by the supplier to increase the intrinsic viscosity and the molecular weight of the PLA. Various CE amounts up to 3 wt.% were used (0.5, 1.5, 2 and 3 wt.%). The nomenclature is PLAXC where X represents the weight percentage of CE (for example PLA1.5C for 1.5 wt.% of CE).

### 2.2. Materials processing

PLA pellets were dried under vacuum for 15 h at 50 °C to remove any moisture excess. The residual moisture content was about 500 ppm (measured by Karl Fischer titration). PLA, CE and CFA were dry-mixed before introduction into the hopper of the extruder. The two following processing steps were implemented for the elaboration of PLA/CE foams.

#### 2.2.1. PLA/CE compounding

A dry blend of PLA/CE was compounded using a twin-screw intermeshing co-rotating extruder (BC21, CLEXTRAL, France) which screw diameter, centerline distance and L/D ratio are equal to 25 mm, 21 mm and 36

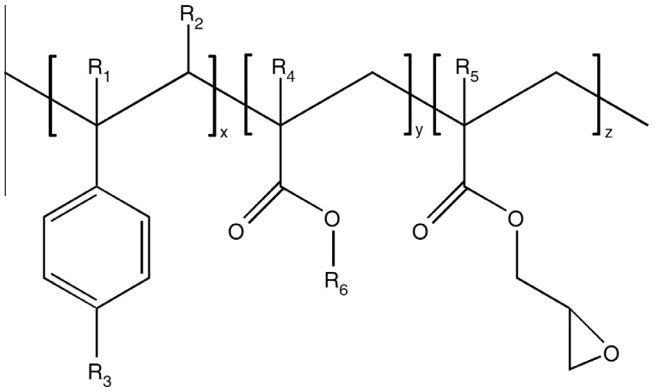


**Fig. 1.** Chemical structure of the multi-functional epoxide-based chain-extender. $R_1$–$R_5$ are H, $CH_3$, an alkyl group or a combination of them; $R_6$ is an alkyl group.

respectively, equipped with a strand die. The temperature control is carried out on 12 zones, the screw speed is set at 250 rpm and the residence time is approximately equal to 1 min. The double-flighted screw profile is given in Fig. 2. Conveying and kneading elements are used in the first four zones of the barrel to facilitate conveying and melting of the PLA/CE blend. Backward-pumping elements are used further downstream in order to separate different procedural zones and to favor homogenization of the blend. At the die exit, the strand is cooled in a water bath and then granulated using a strand cutter. The global flow rate in the twin-screw extruder is set at 4 kg/h.

*2.2.2. PLA/CE foaming*

PLA-based foams were processed using a single-screw extruder (COMPACT – FAIREX Company, France), equipped with a general-purpose screw (30 mm diameter, *L*/*D* ratio 24). The extrusion is done through a flat die having a width of 40 mm and a gap of 1.5 mm. The barrel temperature profiles are given on Table 1. Temperature profile A is used for cellular materials and temperature profile B is used for the bulk materials (non-cellular materials as references). The screw speed is set at 30 rpm. The cooling was carried out by a three-roll calender (HAAKE Tape Postex – Thermo Electron Corporation, Germany) at a controlled temperature of −15 °C using a chill-roll regulation (HAAKE Phoenix II – Thermo Electron Corporation, Germany). The cellular PLA with 0 wt.% CE (PLA0C), whose viscosity is too low, was cooled at a speed of 8.83 rpm instead of 6.7 rpm used for other cellular materials. Similarly, bulk samples (non-cellular) were cooled with a speed of 6.38 rpm. The PLA/CE compound and the CFA are dry-mixed before introduction into the hopper of the extruder. For all materials the weight percentage of CFA was set at 4 wt.%.

**Table 1**
Temperature profiles used for PLA/CE foaming (single screw struder).

| Temperature profile | Temperature (°C) | | | | | |
|---|---|---|---|---|---|---|
| | Barrel (From hopper to die) | | | | | Die |
| | 1 | 2 | 3 | 4 | 5 | 6 |
| A | 130 | 150 | 165 | 165 | 170 | 195 |
| B | 150 | 150 | 160 | 160 | 160 | 160 |

## 3. Methods

*3.1. Solution viscometry*

The solution viscosity of PLA/CE blends was measured at 25 °C, in solution in chloroform (with concentrations ranging from 0.25 to 1 g/dL), using an Ubbelohde capillary viscometer (model 0C), according to ISO 1628-1 standard [36]. The intrinsic viscosity [$\eta$] (Eq. (1)) is determined according to the limit value of the reduced viscosity also called viscosity index I (Eq. (2)) for an infinite dilution. The viscosity-average molecular weight ($M_v$) of the PLA/CE blends was then calculated thanks to the Mark–Houwink–Sakurada equation (Eq. (3)), It is a relationship between the intrinsic viscosity [$\eta$] of the material and $M_v$.

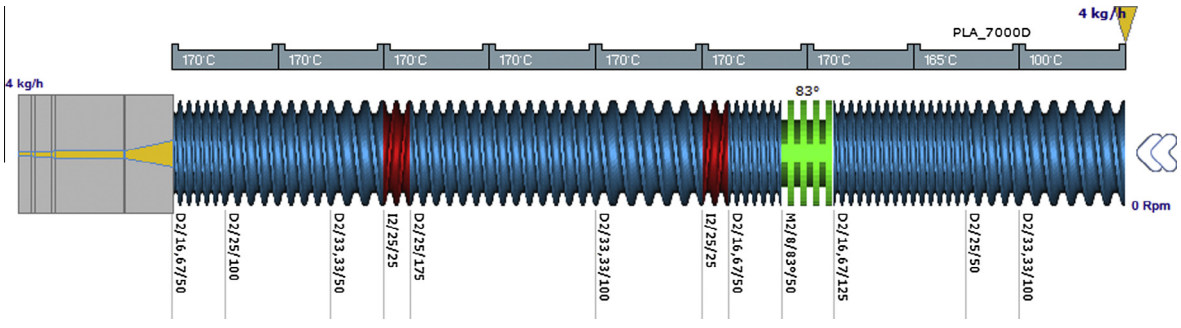


**Fig. 2.** Screw and temperature profile used for PLA/CE twin screw compounding.

$$[\eta] = \lim_{c \to 0}\left(\frac{\eta - \eta_0}{\eta_0 c}\right) \quad (1)$$

$$I = \frac{\eta - \eta_0}{\eta_0 c} \quad (2)$$

$$M_v = \left(\frac{[\eta]}{K}\right)^{\frac{1}{\alpha}} \quad (3)$$

where $K = 4.41 \cdot 10^{-4}$ dL g$^{-1}$ and $\alpha = 0{,}72$ are constants depending on the characteristics of the PLA, chloroform and temperature (25 °C) of the solution [7]. $\eta$ and $\eta_0$ represent the viscosity of the polymer solution and the viscosity of the pure solvent respectively. $c$ is the solution concentration (g dL$^{-1}$)

### 3.2. Thermal analysis: DSC (differential scanning calorimetry) and TGA (thermogravimetric analysis)

The melting ($T_m$) and glass transition temperatures ($T_g$) as well as the degree of crystallinity ($\chi_c$) of PLA/CE blends have been determined by using differential scanning calorimetry (Perkin Elmer Pyris Diamond, USA) under nitrogen atmosphere, during the heating of the samples from 20 to 200 °C at a rate of 10 °C/min. The degree of crystallinity ($\chi_c$) was calculated from the measurements of the melting ($\Delta H_m$) and crystallization ($\Delta H_c$) enthalpies (Eq. (4)).

$$\chi_c = \frac{\Delta H_m - |\Delta H_c|}{93} \times \frac{100}{w} \quad (4)$$

The constant 93 J/g corresponds to the melting enthalpy of 100% crystalline P(L-LA) or P(D-LA) [2,7,37,38] and $w$ is the weight fraction of PLA contained in the blend.

The thermal stability of PLA/CE blends was characterized by thermogravimetry analysis (STA 409C, Netzsch, Germany) under air, between 20 °C and 700 °C, with a heating rate of 5 °C/min.

### 3.3. Rheological properties

Dynamic shear rheological measurements were carried out using a rotational rheometer (ARES, TA Instruments, USA) in oscillatory mode. A parallel-plate (25 mm diameter) geometry was selected for the frequency sweeps under 1% controlled strain. This strain value was first verified to be in the linear viscoelastic domain for all the samples. The angular frequencies were swept from 0.1 to 100 rad s$^{-1}$ at 180 °C with 1.5 mm gap.

### 3.4. Apparent density

The apparent density ($\rho_f$) of PLA/CE foams was estimated from the measurement of the weight ($m$) and the volume ($V$) of a given sample. Samples were cut from the extruded strips. The sample sizes (the nominal size is about 80 × 30 × 1.5 mm$^3$) were measured with a vernier caliper. Their mass (m) was measured using a balance with a precision of 0.01 mg (AT250, Mettler-Toledo AG, Switzerland). The apparent density ($\rho_f$), expressed in kg/m$^3$, is then deduced from Eq. (5). The reported values are the average densities measured on 5 samples.

$$\rho_f = \frac{m}{V} \times 10^6 \quad (5)$$

where

$m$: mass, in grams;

$V$: the geometric volume, in cubic millimetres.

### 3.5. Void fraction

The void fraction ($V_f$) of foams is determined by Eq. (6) from the densities of the extruded neat PLA ($\rho_p$) and of the PLA foam ($\rho_f$).

$$V_f = 100 \quad 1 - \frac{\rho_f}{\rho_p}\Big) \quad (6)$$

### 3.6. Cellular structure of foams

The cellular structure of foams was observed on cryofractured (perpendicularly to the flow direction) extruded parts using environmental scanning electron microscopy (ESEM) (FEI Quanta 200 FEG, FEI, USA), under a pressure of 0.83 Torr and with a magnification of 75. ESEM images, containing approximately 300 cells, were then analyzed using image processing software (Optimas® 6.5, Imasys, USA) The cell size distribution was derived from the determination of the equivalent diameter ($d_i$) which is calculated from the area ($A_i$) of each cell (Eq. (7)). However, this value must be corrected to limit bias related to the finite image frame size. This correction is based on the inclusion probability of the cells into the image frame. For this purpose, the methodology of image frame correction, developed by Miles and Lantuejoul [39,40] was applied. The following data were obtained:

(a) The equivalent diameter (based on a circular shape) of the cells $d_i$ (Eq. (7)).

(b) The number-average diameter $\overline{d_n}$ (Eq. (8)), the size-average diameter $\overline{d_w}$ (Eq. (9)) and the polydispersity index (PDI) of the cells diameter distribution (Eq. (10)). $n_i$ is the number of cells.

(c) The theoretical cell density $N_c$ (Eq. (11)).

(d) The cell-wall thickness $\delta$ (Eq. (12)).

$$d_i = 2\sqrt{A_i/\pi} \quad (7)$$

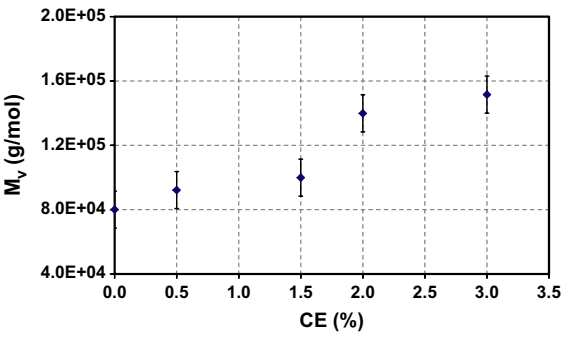


**Fig. 3.** Chain-extender effect on the viscometric average molecular weight ($M_V$) of PLA.

**Table 2**
Chain extender effect on the phase transitions and degree of crystallinity of PLA ($T_g$: glass transition temperature; $T_m$: melting temperature; $T_c$: cold crystallization temperature; $X_c$: degree of crystallinity).

| Materials | CE (%) | $T_g$ (°C) | $T_m$ (°C) | $T_C$ (°C) | $\chi_C$ (%) |
|---|---|---|---|---|---|
| PLA0C | 0 | 62.7 ± 1.5 | 153.3 ± 0.3 | – | 2.3 ± 1.20 |
| PLA0.5C | 0.5 | 63.6 ± 0.1 | 153.2 ± 0.9 | 128.6 ± 1.9 | 0.0 ± 0.3 |
| PLA1.5C | 1.5 | 63.1 ± 0.3 | 151.9 ± 0.3 | 124.9 ± 0.4 | 0.0 ± 1.0 |
| PLA2C | 2 | 63.0 ± 0.7 | 151.2 ± 0.9 | 123.2 ± 1.1 | 0.0 ± 1.2 |
| PLA3C | 3 | 63.0 ± 0.7 | 151.3 ± 1.2 | 122.9 ± 1.7 | 0.0 ± 1.6 |

$$\overline{d_n} = \frac{\sum(d_i n_i)}{\sum n_i} \tag{8}$$

$$\overline{d_w} = \frac{\sum(d_i^2 n_i)}{\sum(d_i n_i)} \tag{9}$$

$$\mathrm{PDI} = \frac{\overline{d_n}}{\overline{d_w}} \tag{10}$$

In the case of $N_c$ (Eq. (11)) and $\delta$ (Eq. (12), calculations are based on the assumption that the materials contain only spherical cells [17,41–44]. According to Gosselin et al. [45], the cells are not truly spherical or isotropic in the case of extrusion and injection foaming because of the extension in the flow direction, induced by the shear and elongation stresses. Most realistic models take into account cell deformation in the flow direction, assuming that the cells are ellipsoids of revolution. As a result, several cross-sections are needed to estimate the three axes of the ellipsoid which is a tedious task [45–47]. Therefore, as most authors [17,41–44], the simplest model assuming that the cells are perfectly spherical was considered here.

$$N_c = \frac{1 - \left(\rho_f/\rho_p\right)}{\left(\pi \overline{d_n}^3/6\right)} \tag{11}$$

$$\delta = \overline{d_n}\left(\frac{1}{\sqrt{\left(1 - \frac{\rho_f}{\rho_p}\right)}} - 1\right) \tag{12}$$

The relative uncertainty measurement on the average cell size $\overline{d_n}$, the cell density $N_c$ and the cell-wall thickness $\delta$, is about 2%, 7% and 2% respectively. These values are determined by processing 3 times consecutively a batch image. The distribution of cell size is adjusted by a log-normal law according to maximum-likelihood estimation among several standard mathematical laws.

**Table 3**
Chain extender effect on the thermal stability of PLA ($T_{onset}$ and $T_{end}$: onset and end degradation temperature respectively; $T_{peak}$: temperature at the peak of the 1st derivative of the weight loss curve).

| Materials | CE (%) | $T_{onset}$ (°C) | $T_{peak}$ (°C) | $T_{end}$ (°C) |
|---|---|---|---|---|
| PLA0C | 0 | 329 ± 0.4 | 347 ± 0.3 | 357 ± 0.2 |
| PLA05C | 0.5 | 327 ± 0.3 | 346 ± 0.2 | 356 ± 0.2 |
| PLA1.5C | 1.5 | 329 ± 0.0 | 347 ± 0.0 | 356 ± 1.2 |
| PLA2C | 2 | 328 ± 0.6 | 347 ± 0.6 | 356 ± 0.7 |
| PLA3C | 3 | 328 ± 0.3 | 346 ± 0.5 | 356 ± 0.8 |

### 3.7. Open cell content

The open cells content ($C_o$) of PLA/CE foams was quantified (Eq. (13)) using a helium pycnometer, (Accupyc 1330, Micromeritics, USA). The tests were performed on samples of size around 40 × 30 × 1.50 mm$^3$. The result is an average value obtained by testing three samples.

$$C_0 = 100\frac{V_g - V_r}{V_g} \tag{13}$$

where

$V_g$: Geometric volume determined by vernier caliper measurement,

$V_r$: The actual geometric volume determined by pycnometry.

### 3.8. Uniaxial tensile properties

The mechanical properties (stress and elongation at yield and break) under tension were measured according to ISO 527-2 [48]. Samples dimensions did not permit to evaluate the Young's modulus. The samples (5A type) were collected from extruded parts, parallel to the extrusion direction, and conditioned at least 3 days at room temperature (23 °C). The tests were performed using a tensile testing machine (Z010, ZWICK, Germany), equipped with a 0.5 kN capacity load cell and with a crosshead speed of 2 mm/min. The reported results are the average from 10 samples measurements.

## 4. Results and discussions

### 4.1. Characterization of PLA/CE blends prior to extrusion foaming

#### 4.1.1. Viscometric average molecular weight

Fig. 3 shows the sharp increase of the viscometric average molecular weight induced by the incorporation fraction of CE (+89% of increase compared to neat PLA when the CE content is set to 3 wt.%). This result is consistent

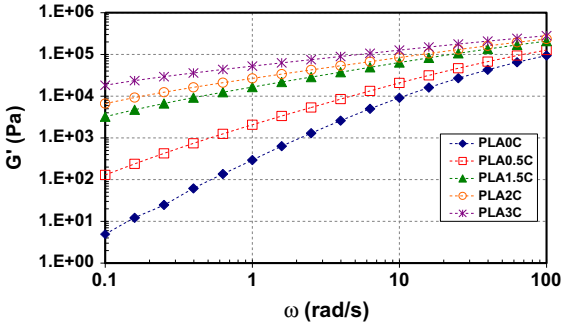


**Fig. 4.** Storage modulus $G'$ as a function of angular frequency ($\omega$) for PL/CE at 180 °C, 1% strain and 0.1–100 rad/s.

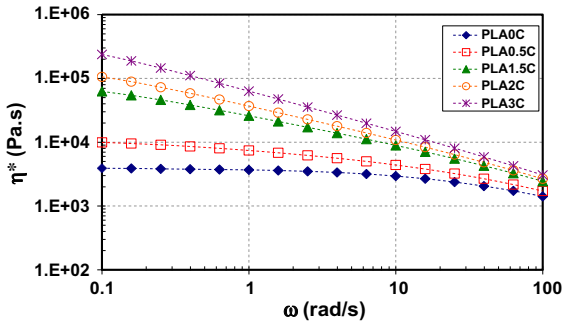


**Fig. 5.** Complex viscosity ($\eta^*$) as a function of angular frequency ($\omega$) for PLA CE at 180 °C, 1% strain and 0.1–100 rad/s.

with those reported by other works which attribute them to extension and chains branching mechanisms [4,29,49].

*4.1.2. Phase transitions and degree of crystallinity*

Table 2 shows that the incorporation of chain extender has no significant effect either on the melting and glass transition temperatures or on the degree of crystallinity. Same observations were noted by other authors [49]. However, a cold crystallization ($T_c$) phenomenum occurs as soon as CE is incorporated within PLA. This cold crystallization seems to decrease from 129 °C to 123 °C when the CE content increases from 0.5 to 3 wt.%. This result could be related to a better reorganization (chain-branching) of PLA chains in presence of CE [4]. Moreover, the CE incorporation does not affect PLA thermal stability (Table 3) unlike conclusions from Pilla et al. [4], but these authors used higher CE contents (8 wt.%) and observed only a slight improvement of the thermal stability (4 °C).

*4.1.3. Rheological properties*

The effect of the chain extender incorporation on the molecular weight and the branching is confirmed by the rheological behavior analysis of the samples containing 0–3 wt.% of CE (Figs. 4 and 5). Results show first a significant increase (four decades for 3 wt.% CE) of the storage modulus $G'$ at low angular frequency (Fig. 4), whereas this modulus is rather slightly modified at higher angular frequency (100 rad/s). Moreover, a significant increase (two decades for 3 wt.% CE) of the complex viscosity $\eta^*$ is also observed at low angular frequency, associated to a dramatic shift to the lower angular frequencies of the newtonian-pseudoplastic transition. The effect of the CE addition is only slight at high angular frequency. All these phenomena are amplificated with the increase in the CE content.

This change in the rheological behavior is consistent with the one of the viscometric-average molecular weight previously presented (Fig. 3) [29] and was already observed by Di et al. [29] on reactively modified PLA and Villalobos et al. [30] on PBT/PA blended using a chain extender.

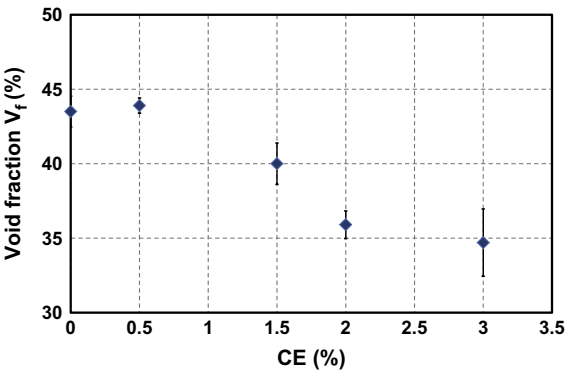


**Fig. 6.** Effect of the CE incorporation fraction on the void fraction of PLA foams.

*4.2. Influence of the chain extender content on PLA-based foams properties*

*4.2.1. Void fraction of PLA-based foams*

Fig. 6 shows that, except for the lowest CE content (0.5 wt.%), the addition of the chain extender reduces the ability to the expansion of the PLA, leading to a reduction of the void fraction of the foams. That is to correlate to the increase in the viscosity and in the molecular weight of the materials, which inhibits the growth of the cells.

*4.2.2. Cellular structure of PLA-based foams*

Fig. 7 and Table 4 show significant differences in the cell size in presence of CE.

Up to 2 wt.% of CE, the more important the CE weight fraction the finer the cell structure (smaller cell size $\overline{d_n}$ and higher cell density $N_c$ as given in Table 4). The increase in the molecular weight and viscosity handicaps the cell growth [4] thus resulting in smaller cells. In this range of CE weight content a possible melt strength enhancement or strain hardening could result in domination of cell nucleation over cell growth. For higher CE content (3 wt.%) an increase in the cell size and a decrease in the cell density is observed whereas the void fraction is quite similar to 2 wt.% CE content formulation. We assume that the gas bubbles nucleation rate is mainly determined by the distribution of the nucleating particles (included in the CFA), the pressure drop at the extruder die exit and the surface tension of the polymer melt [50]. In order to comment the differences between 2 wt.% and 3 wt.% CE content formulations and considering separately each of the three prevailing factors we can assume that the distribution of nucleating particles is the same (CFA content is identical, 4 wt.%), the pressure drops near the die exit are quite identical (the average shear rate in the final part of the die was estimated at 150 $s^{-1}$ and Fig. 5 shows quite no difference in viscosity and then in pressure drop for this shear rate between 2 and 3 wt.% CE content). The last factor concerns the surface tension of the polymer. Yet several papers pointed out a correlation between chain branching or extension and a change in the surface tension of a polymer. Chain branching or extension generally produces an increase in the surface tension of the polymer which handicaps the nucleation of gas bubbles, thus resulting in a decrease in the cell density and an increase in their average

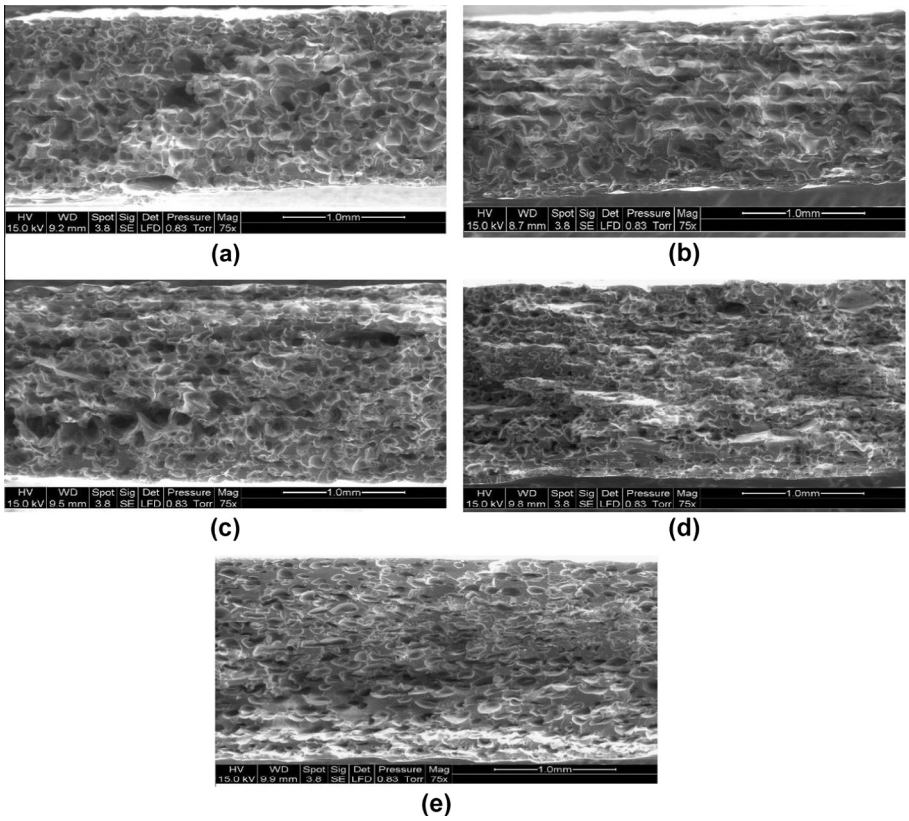


**Fig. 7.** PLA morphological structure as a function of the weight content of CE ((a) PLA0C, (b) PLA0.5C; (c) PLA1.5C; (d) PLA2C; (e) PLA3C).

**Table 4**
Cell sizes ($\overline{d_w}$ and $\overline{d_n}$) and density ($N_c$), polydispersity index of cell size distribution (PDI), cell-wall thickness ($\delta$) as a function of the weight fraction of CE.

| Materials | CE (%) | $\overline{d_n}$ (μm) | $\overline{d_w}$ (μm) | PDI | $N_c$ (cells/cm$^3$) $10^5$ | $\delta$ (μm) |
|---|---|---|---|---|---|---|
| PLA0C | 0 | 106 ± *2* | 131 ± *2* | 0.81 ± *0.01* | 6.98 ± *0.48* | 55 ± *1* |
| PLA0.5C | 0.5 | 97 ± *2* | 114 ± *2* | 0.85 ± *0.01* | 9.20 ± *0.64* | 49 ± *1* |
| PLA1.5C | 1.5 | 90 ± *2* | 103 ± *1* | 0.88 ± *0.01* | 10.50 ± *0.73* | 52 ± *1* |
| PLA2C | 2 | 64 ± *1* | 71 ± *1* | 0.89 ± *0.01* | 26.60 ± *1.85* | 43 ± *1* |
| PLA3C | 3 | 84 ± *2* | 96 ± *1* | 0.88 ± *0.01* | 11.04 ± *0.77* | 59 ± *1* |

Values in italic correspond to standard deviations.

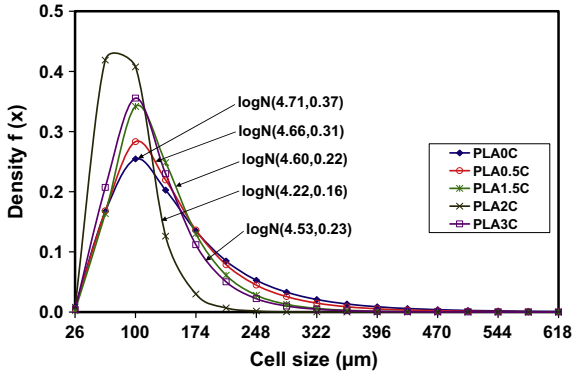


**Fig. 8.** Comparison of the weight content effect of chain extender in the PLA on the width of the cells diameter distribution by a log-normal distribution fit log$N$ (mean $\mu$, variance $\sigma^2$).

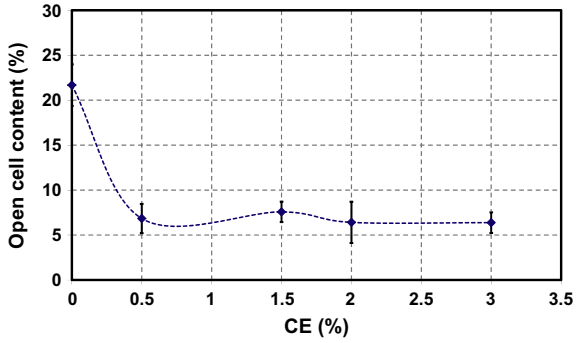


**Fig. 9.** Evolution of the open cells ($C_o$) as a function of the weight content of CE of the various PLA-based foams.

**Table 5**
Tensile properties as a function of the CE weight ratio of PLA based foams – ($\sigma_y$ and $\varepsilon_y$: stress and strain at yield; $\sigma_r$ et $\varepsilon_r$: stress and strain at break).

| Materials | CE (%) | $V_f$ (%) | $\sigma_y$ (MPa) | $\varepsilon_y$ (%) | $\sigma_r$ (MPa) | $\varepsilon_r$ (%) |
|---|---|---|---|---|---|---|
| PLA0C | 0 | 43 ± *1* | 17.8 ± *1.4* | 7.6 ± *1.0* | 16.3 ± 1.3 | 8.3 ± *1.1* |
| PLA0.5C | 0.5 | 44 ± *1* | 17.0 ± *0.5* | 8.2 ± *0.5* | 12.9 ± 1.9 | 13.1 ± *1.8* |
| PLA1.5C | 1.5 | 40 ± *1* | 17.8 ± *0.9* | 8.3 ± *0.6* | 12.4 ± 0.9 | 12.7 ± *2.0* |
| PLA2C | 2 | 36 ± *1* | 22.5 ± *1.3* | 8.0 ± *0.9* | 16.3 ± 2.6 | 12.4 ± *1.5* |
| PLA3C | 3 | 35 ± *2* | 27.5 ± *1.9* | 8.9 ± *0.8* | 16.0 ± 3.5 | 13.7 ± *2.8* |

Values in italic correspond to standard deviations.

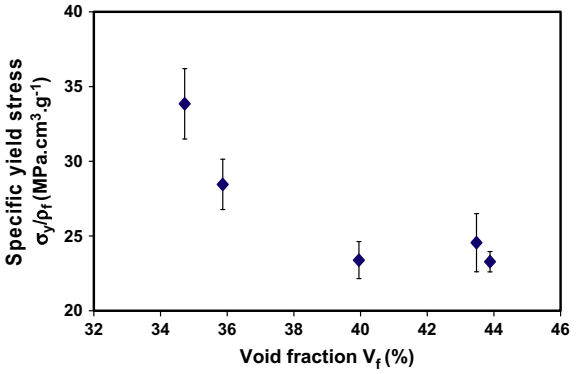


**Fig. 10.** Evolution of the specific tensile yield stress as a function of the void fraction of cellular PLA at various CE weight ratios.

diameter [51–53]. Moreover, the dependence of the cell-wall thickness ($\delta$) as a function of the CE weight fraction is not monotonous. Finally, the addition of the chain extender tends to homogenize the cell size distribution (lower polydispersity index and more narrow size distribution as can be seen from the variance values (Fig. 8)).

*4.2.3. Open cell content of PLA-based foams*

The addition of the chain extender leads to a very significant reduction in the volume percentage of open cells $C_o$ (Fig. 9). This can be related to the increase of the viscosity and the storage modulus induced by the presence of the chain extender that hinders the cell growth and prevents the cell wall failure by overstretching. This is consistent with the results obtained by other authors on linear and branched PLA [54,55]. Indeed, the open cells ratio decreases from 21% to about 6% this last value being quite independent of the CE weight content.

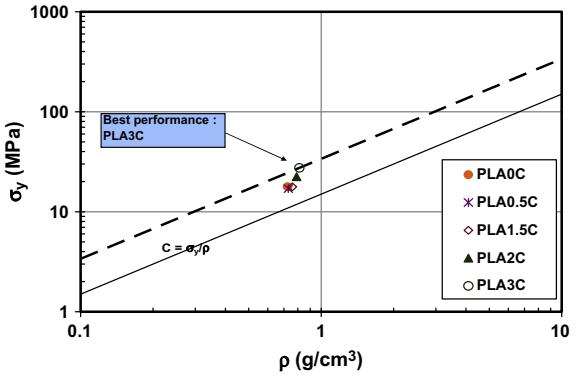


**Fig. 11.** Yield tensile stress ($\sigma_y$) as a function of density ($\rho$) at various CE weight ratios in log–log representation (---- selection line for constant ratio $\sigma_y/\rho$; – – – position of the selection line for the best efficient material).

*4.2.4. Mechanical properties of PLA-based foams*

The void content decrease leads to an increase of the tensile yield stress of PLA-based foams (Table 5) particularly for 2 and 3 wt.% of CE. The effect on the tensile stress at break is not significant, given the standard deviations. The chain extender incorporation has quite no effect on the strain at break. These trends are maintained for the specific yield stress ($\sigma_y/\rho_f$) and are directly related to the evolution of void fractions (Fig. 10).

Finally, the concept of performance index [56] was used to monitor the evolution of the tensile yield stress/density ratio (called specific tensile yield stress) of different materials and to optimize their choice on a mechanical performance basis. Indeed, a performance index is associated with a function (for example efficiency under uniaxial tensile stress), an objective (for example minimization of the mass of a beam of any cross section but constant over its length), a constraint (for example stress in the beam does not exceed the tensile yield stress $\sigma_y$ and the length of the beam is fixed) and a set of free variables and specified variables (geometry of the section of the beam). Under these conditions (cited as example), the performance index to maximize can be derived as $\sigma_y/\rho_f$ (called specific yield stress in our case). $\rho_f$ is the density of the material. This index can then be used to determine unambiguously the best material for a given function (here a beam under axial loading).

In this context, the PLA3C shows the highest performance index for the function described above (Fig. 11 shows a chart representing $\sigma_y$ vs. $\rho_f$ in log–log scales and the selection line of slope 1 which has to be upward shifted until the last experimental point is reached). PLA3C is therefore the best choice among all the cellular PLA materials produced with various chain extender weight contents (Fig. 11), because it is the only one tangent to the selection line in the uppermost position.

## 5. Conclusions

The influence of an epoxy-based chain-extender (CE) within PLA on the characteristics of cellular materials has been highlighted. The effects on expansion, cell morphology and mechanical characteristics were considered. While the study shows that the presence of CE induces a decrease in void fraction of PLA foams except for a low CE content (0.5 wt.%) for which the void fraction remains

unchanged. It leads to a decrease in cells size (from 106 to 84 μm) and open cell content (from 22% to about 6%) an increase in tensile properties (from 17.8 to 27.5 MPa for yield stress). The study showed also that the PLA3C is the one which has the largest specific yield ratio which could be of interest for structural applications (in tension or compression) of this kind of material. Finally, whereas no improvement in void fraction is obtained, chain-extenders could be useful to handle the cell morphology in order to obtain finer and more homogeneous cells.

## References


[1] Julien JM, Bénézet JC, Lafranche E, Quantin JC, Bergeret A, Lacrampe MF, et al. Development of poly(lactic acid) cellular materials: physical and morphological characterizations. Polymer 2012;53(25):5885–95. http://dx.doi.org/10.1016/j.polymer.2012.10.005.

[2] Martin O, Avérous L. Poly(lactic acid): plasticization and properties of biodegradable multiphase systems. Polymer 2001;42(14):6209–19. http://dx.doi.org/10.1016/S0032-3861(01)00086-6.

[3] Nugroho P, Mitomo H, Yoshii F, Kume T. Degradation of poly(-lactic acid) by γ-irradiation. Polym Degrad Stabil 2001;72(2):337–43. http://dx.doi.org/10.1016/S0141-3910(01)00030-1.

[4] Pilla S, Kramschuster A, Yang L, Lee J, Gong S, Turng L-S. Microcellular injection-molding of polylactide with chain-extender. Mater Sci Eng: C 2009;29(4):1258–65. http://dx.doi.org/10.1016/j.msec.2008.10.027.

[5] Chandra R, Rustgi R. Biodegradable polymers. Prog Polym Sci 1998;23(7):1273–335. http://dx.doi.org/10.1016/S0079-6700(97)00039-7.

[6] Matuana LM. Solid state microcellular foamed poly(lactic acid): morphology and property characterization. Bioresour Technol 2008;99(9):3643–50. http://dx.doi.org/10.1016/j.biortech.2007.07.062.

[7] Lim LT, Auras R, Rubino M. Processing technologies for poly(lactic acid). Prog Polym Sci 2008;33(8):820–52. http://dx.doi.org/10.1016/j.progpolymsci.2008.05.004.

[8] Bastioli C. Handbook of biodegradable polymers. Smithers Rapra Technology; 2005.

[9] Auras R, Harte B, Selke S. An overview of polylactides as packaging materials. Macromol Biosci 2004;4(9):835–64. http://dx.doi.org/10.1002/mabi.200400043.

[10] Kale G, Auras R, Singh SP, Narayan R. Biodegradability of polylactide bottles in real and simulated composting conditions. Polym Test 2007;26(8):1049–61. http://dx.doi.org/10.1016/j.polymertesting.2007.07.006.

[11] Bleach NC, Nazhat SN, Tanner KE, Kellomäki M, Törmälä P. Effect of filler content on mechanical and dynamic mechanical properties of particulate biphasic calcium phosphate–polylactide composites. Biomaterials 2002;23(7):1579–85. http://dx.doi.org/10.1016/S0142-9612(01)00283-6.

[12] Heino A, Naukkarinen A, Kulju T, Törmälä P, Pohjonen T, Mäkelä EA. Characteristics of poly(L-)lactic acid suture applied to fascial closure in rats. J Biomed Mater Res 1996;30(2):187–92. http://dx.doi.org/10.1002/(SICI)1097-4636(199602)30:2<187::AID-JBM8>3.0.CO;2-N.

[13] Luciano RM, Zavaglia CAC, Duek EAR, Alberto-Rincon MC. Synthesis and characterization of poly(L-lactic acid) membranes: studies in vivo and in vitro. J Mater Sci Mater Med 2003;14(1):87–94. http://dx.doi.org/10.1023/A:1021509722296.

[14] Itoh E, Matsuda S, Yamauchi K, Oka T, Iwata H, Yamaoka Y, et al. Synthetic absorbable film for prevention of air leaks after stapled pulmonary resection. J Biomed Mater Res 2000;53(6):640–5. http://dx.doi.org/10.1002/1097-4636(2000)53:6<640::AID-JBM4>3.0.CO;2-L.

[15] Pego AP, Siebum B, Van Luyn MJA, Gallego y Van Seijen XJ, Poot AA, Grijpma DW, et al. Preparation of degradable porous structures based on 1,3-trimethylene carbonate and D,L-lactide (co) polymers for heart tissue engineering. Tissue Eng 2003;9(5):981–94. http://dx.doi.org/10.1089/10763270332249562.

[16] Graupner N, Herrmann AS, Müssig J. Natural and man-made cellulose fibre-reinforced poly(lactic acid) (PLA) composites: an overview about mechanical characteristics and application areas. Compos Part A – Appl Sci 2009;40(6–7):810–21. http://dx.doi.org/10.1016/j.compositesa.2009.04.003.

[17] Klempner D, Sendijarevic V. Handbook of polymeric foams and foam technology. 2nd ed. Munich: Hanser Gardner publications, Carl Hanser Verlag; 2004.

[18] Les matériaux en mousse et leurs applications industrielles. Editeur: Innovation 128 TechTendances juillet; 1997. P. 150.

[19] Lee ST. Foam extrusion: principles and practice. Lancaster, PA, USA: Technomic Publishing Company; 2000. P. 368.

[20] Greco A, Maffezzoli A, Manni O. Development of polymeric foams from recycled polyethylene and recycled gypsum. Polym Degrad Stabil 2005;90(2):256–63. http://dx.doi.org/10.1016/j.polymdegradstab.2005.01.026.

[21] Di Y, Iannace S, Di Maio E, Nicolais L. Poly(lactic acid)/organoclay nanocomposites: thermal, rheological properties and foam processing. J Polym Sci Pol Phys 2005;43(6):689–98. http://dx.doi.org/10.1002/polb.20366.

[22] Pagnoulle C, Stassin F, Chapelle G, Jerome R. Method for preparing biodegradable polyester foams, polyester foams obtained thereby, and the use thereof. Belgium, WIPO patent application WO/2004/108806; 2004.

[23] Nijenhuis AJ, Grijpma DW, Pennings AJ. Crosslinked poly(l-lactide) and poly(ε-caprolactone). Polymer 1996;37(13):2783–91. http://dx.doi.org/10.1016/0032-3861(96)87642-7.

[24] Nagasawa N, Kaneda A, Kanazawa S, Yagi T, Mitomo H, Yoshii F, et al. Application of poly(lactic acid) modified by radiation crosslinking. Nucl Instrum Meth B: Beam Interact Mater Atoms 2005;236(1–4):611–6. http://dx.doi.org/10.1016/j.nimb.2005.04.052.

[25] Zaidi L, Bruzaud S, Kaci M, Bourmaud A, Gautier N, Grohens Y. The effects of gamma irradiation on the morphology and properties of polylactide/cloisite 30B nanocomposites. Polym Degrad Stabil 2013;98:348–55. http://dx.doi.org/10.1016/j.polymdegradstab.2012.09.014.

[26] Cairns ML, Dickson GR, Orr JF, Farrar D, Hawkins K, Buchanan FJ. Electron-beam treatment of poly(lactic acid) to control degradation profiles. Polym Degrad Stabil 2011;96:76–83. http://dx.doi.org/10.1016/j.polymdegradstab.2010.10.016.

[27] Grimes E, Keeley S. Foaming of PLA – the use of melt strength enhancers to achieve lower density foams produced by chemical blowing agents. Rubber World 2010;243(1). pp. 28–29,33.

[28] Li BH, Yang MC. Improvement of thermal and mechanical properties of poly(L-lactic acid) with 4,4-methylene diphenyl diisocyanate. Polym Adv Technol 2006;17:439–43. http://dx.doi.org/10.1002/pat.731.

[29] Di Y, Iannace S, Di Maio E, Nicolais L. Reactively modified poly(lactic acid): properties and foam processing. Macromol Mater Eng 2005;290(11):1083–90. http://dx.doi.org/10.1002/mame.200500115.

[30] Villalobos M, Awojulu A, Greeley T, Turco G, Deeter G. Oligomeric chain extenders for economic reprocessing and recycling of condensation plastics. Energy 2006;31(15):3227–34. http://dx.doi.org/10.1016/j.energy.2006.03.026.

[31] Bikiaris DN, Karayannidis GP. Thermomechanical analysis of chain-extended PET and PBT. J Appl Polym Sci 1996;60(1):55–61. http://dx.doi.org/10.1002/(SICI)1097-4628(19960404)60:1<55::AID-APP7>3.0.CO;2-U.

[32] Bikiaris DN, Karayannidis GP. Chain extension of polyesters PET and PBT with N, N′-bis(glycidyl ester) pyromellitimides. I. J Polym Sci Polym Chem 1995;33(10):1705–14. http://dx.doi.org/10.1002/pola.1995.080331017.

[33] Bikiaris DN, Karayannidis GP. Chain extension of polyesters PET and PBT with two new diimidodiepoxides. II. J Polym Sci Polym Chem 1996;34(7):1337–42. http://dx.doi.org/10.1002/(SICI)1099-0518(199605)34:7<1337::AID-POLA22>3.0.CO;2-9.

[34] Inata H, Matsumura S. Chain extenders for polyesters. V. Reactivities of hydroxyl-addition-type chain extender; 2,2′-bis(4h-3,1-benzoxazin-4-one). J Appl Polym Sci 1987;34(7):2609–17. http://dx.doi.org/10.1002/app.1987.07034072.

[35] Dhavalikar R, Xanthos M. Parameters affecting the chain extension and branching of PET in the melt state by polyepoxides. J Appl Polym Sci 2003;87(4):643–52. http://dx.doi.org/10.1002/app.11425.

[36] Plastics – determination of the viscosity of polymers in dilute solution using capillary viscometers – Part 1: General principles EN ISO 1628-1:2009.

[37] Avérous L, Mohamed Naceur B, Alessandro G. Polylactic acid: synthesis, properties and applications. monomers, polymers and composites from renewable. Resources 2008:433–50.

[38] Södergård A, Stolt M. Properties of lactic acid based polymers and their correlation with composition. Prog Polym Sci 2002;27(6):1123–63. http://dx.doi.org/10.1016/S0079-6700(02)00012-6.

[39] Coster M, Chermant JL. Précis d'analyse d'images, Paris: ed. Presses du CNRS, 1989:560.
[40] Avérous L, Quantin JC, Lafon D, Crespy A. Granulometric characterization of short fiberglass in reinforced polypropylene. Relation to processing conditions and mechanical properties. Int J Polym Anal Chem 1995;1(4):339–47. http://dx.doi.org/10.1080/10236669508233886.
[41] Tsivintzelis I, Pavlidou E, Panayiotou C. Biodegradable polymer foams prepared with supercritical $CO_2$–ethanol mixtures as blowing agents. J Supercrit Fluid 2007;42(2):265–72. http://dx.doi.org/10.1016/j.supflu.2007.02.009.
[42] Alavi SH, Gogoi BK, Khan M, Bowman BJ, Rizvi SSH. Structural properties of protein-stabilized starch-based supercritical fluid extrudates. Food Res Int 1999;32(2):107–18. http://dx.doi.org/10.1016/S0963-9969(99)00063-0.
[43] Ema Y, Ikeya M, Okamoto M. Foam processing and cellular structure of polylactide-based nanocomposites. Polymer 2006;47(15):5350–9. http://dx.doi.org/10.1016/j.polymer.2006.05.050.
[44] Gendron R. Thermoplastic foam processing: principles and development. CRC Press; 2004.
[45] Gosselin R, Rodrigue D. Cell morphology analysis of high density polymer foams. Polym Test 2005;24(8):1027–35. http://dx.doi.org/10.1016/j.polymertesting.2005.07.005.
[46] Vázquez MO, Ramírez-Arreola DE, Bernache J, Gómez C, Robledo-Ortiz JR, Rodrigue D, et al. Using chitosan as a nucleation agent in thermoplastic foams for heavy metal adsorption. Macromol Symp 2009;283–284(1):152–8. http://dx.doi.org/10.1002/masy.200950920.
[47] Sahagun CZ, González-Núñez R. Morphology of extruded PP/HDPE foam blends. J Cell Plast 2006;42:469–85. http://dx.doi.org/10.1177/0021955X06063521.
[48] Plastics – determination of tensile properties – Part 2: Test conditions for molding and extrusion plastics ISO 527–2:1996.
[49] Pilla S, Kim SG, Auer GK, Gong S, Park CB. Microcellular extrusion-foaming of polylactide with chain-extender. Polym Eng Sci 2009;49(8):1653–60. http://dx.doi.org/10.1002/pen.21385.
[50] Stange J, Münstedt H. Effect of long-chain branching on the foaming of polypropylene with azodicarbonamide. J Cell Plast 2006;42:445–67. http://dx.doi.org/10.1177/0021955X06063520.
[51] Nofar M, Park CB. Poly (lactic acid) foaming. Prog Polym Sci 2014;39(10):1721–41. http://dx.doi.org/10.1016/j.progpolymsci.2014.04.001.
[52] Jacobs K, Hall D. Chain extenders improve processing of PLA biopolymers. Bioplast Mag 2008;3:34–6.
[53] Allan GG, Neogi AN. Copolymer characterization by surface tension. J Appl Polym Sci 1970;14:999–1005. http://dx.doi.org/10.1002/app.1970.070140410.
[54] Wang J. Rheology of foaming polymers and its influence on microcellular processing. Ph.D. thesis, Canada: Toronto University; 2009.
[55] Wang J. Continuous processing of low-density, microcellular poly(lactic acid) foams with controlled cell morphology and crystallinity. Chem Eng Sci 2012;75:390–9. http://dx.doi.org/10.1016/j.ces.2012.02.051.
[56] Ashby MF. Materials selection in mechanical design. 2nd edition. England: Department of Engineering, Cambridge University; 1999.